Biomaterials 31 (2010) 1699–1706

Contents lists available at ScienceDirect

Biomaterials

journal homepage: www.elsevier.com/locate/biomaterials

Poly(L-lysine) nanostructured particles for gene delivery and hormone stimulation

Xin Zhang [a,1], Mustapha Oulad-Abdelghani [b,1], Alexander N. Zelkin [c], Yajun Wang [c], Youssef Haîkel [d], Didier Mainard [e], Jean-Claude Voegel [a], Frank Caruso [c,**], Nadia Benkirane-Jessel [a,e,*]

[a] Institut National de la Santé et de la Recherche Médicale, INSERM, Unité 977, Faculté de Médecine, 11 Rue Humann, 67085 Strasbourg Cedex, France
[b] Institut de Génétique et de Biologie Moléculaire et Cellulaire (IGBMC), Institut Clinique de la Souris (ICS), Centre National de la Recherche Scientifique (CNRS)/INSERM/ULP, Collège de France, BP 10142, Strasbourg Cedex 67404, France
[c] Centre for Nanoscience and Nanotechnology, Department of Chemical and Biomolecular Engineering, The University of Melbourne, Victoria 3010, Australia
[d] Faculté de Chirurgie Dentaire de l'Université Louis Pasteur (ULP), Strasbourg Cedex 67000, France
[e] Hôpital Central, «CHIRURGIE ORTHOPEDIQUE ET TRAUMATOLOGIE» 29 Avenue du Maréchal de Lattre de Tassigny, Nancy 54000, France

ARTICLE INFO

Article history:
Received 23 September 2009
Accepted 13 November 2009
Available online 1 December 2009

Keywords:
Mesoporous silica (MS)
Poly (L-lysine) replica particles (PLL_{RP})
Gene delivery
Hormone stimulation

ABSTRACT

In this work, we designed replica particles based on poly (L-lysine) (PLL) polymers crosslinked via a homobifunctional linker to support coadsorption of a plasmid DNA and a peptide hormone for concurrent transfection and induction of a cellular function. PLL replica particles (PLL_{RP}) were prepared by infiltrating polymer into mesoporous silica (MS) particles, crosslinking the adsorbed chains by using a homobifunctional crosslinker and finally removing the template particles. Moreover, we verified their cytotoxicity. Furthermore, based on this PLL_{RP} gene delivery system, we simultaneously evaluated the melanin stimulation and gene expression in these cells by fluorescence microscopy. To further understand the bi-functionality, we labeled the SPT7pTL and PGA-α-MSH with YOYO-1 and Rhodamine, respectively, to follow its intracellular pathway by confocal microscopy. Our data suggests that the PLL_{RP} is a promising vector for gene therapy and hormone stimulation.

1. Introduction

Modern drug delivery relies on the use of drug carrier vehicles that facilitate the delivery of cargo to the target cells, tissues and organs. Examples of carriers include polymers [1], micelles [2], liposomes [3], solid nano- and microparticles [4], polymer capsules [5], and other macromolecular and supramolecular assemblies. Advantages of carrier vehicles include shielding the drug from degradation by the body and reducing potential toxic effects of the drug. Additionally, for hydrophobic water insoluble therapeutics carrier vehicles markedly increase the deliverable payload. Targeted delivery of the drug is also made possible by the attachment of ligands that interact with specific receptors. Recently, we reported the preparation of colloidal drug carriers via infiltration of polymers into sacrificial porous template particles [6–8]. Crosslinking of the adsorbed polymer chains and template removal yields polymer hydrogel replica particles. This approach has been shown to be versatile in terms of polymer types and crosslinking strategies, and accommodates the use of biodegradable polypeptides and linkages to facilitate biomedical applications of the replica particles.

During the past decade, gene therapy has become a worldwide research focus and has been advanced considerably. The main objective in gene therapy is constructing an efficient gene delivery system able to transfer the therapeutic DNA to the targeted tissues and cells. However, despite extensive research, the development of an efficient and safe gene delivery system remains a main challenge for gene therapy. Poly (L-lysine) (PLL) polymers are one of the first cationic polymers used for gene transfer [9]. Currently, PLL has been widely used as a non-viral gene vector. They are polypeptides with amino-acid lysine as a repeat unit and are biodegradable. This property is very useful for *in vivo* applications [10]. Nevertheless, PLL shows a low level of transfection efficiency, primarily owing to the lack of rapid release of PLL/DNA complexes from endosomes [11]. Moreover, PLL suffers from immunogenicity and toxicity caused by its amino-acid backbone [12].

Polymer replica particles are well suited for the adsorption and coadsorption of therapeutics for their concurrent delivery. Specifically, in this work we designed replica particles based on PLL crosslinked via a homobifunctional linker to support coadsorption

* Corresponding author. Institut National de la Santé et de la Recherche Médicale, INSERM, Unité 977, Faculté de Médecine, 11 Rue Humann, 67085 Strasbourg Cedex, France. Fax: +33 3 90243379.
** Corresponding author. Fax: +61 3 83444153.
E-mail addresses: fcaruso@unimelb.edu.au (F. Caruso), nadia.jessel@medecine.u-strasbg.fr, nadia.jessel@odonto-ulp.u-strasbg.fr (N. Benkirane-Jessel).
[1] Both authors contributed equally to this work.

0142-9612/$ – see front matter © 2009 Elsevier Ltd. All rights reserved.
doi:10.1016/j.biomaterials.2009.11.032

of a plasmid DNA and a peptide hormone for concurrent transfection and induction of a cellular function. We outline the preparation of the PLL replica particles (PLL_{RP}), verify their cytotoxicity, and demonstrate their successful use as colloidal carriers for the concurrent gene and drug delivery.

To investigate the gene expression and hormone simulation, we chose SPT7pTL, a vector expressing the human SPT7 nuclear transcription factor, and alpha-melanocyte-stimulating hormone (α-MSH) as a reporter hormone. B16-F1 cells were used because these cells respond specifically to α-MSH. α-MSH is a potent stimulator of melanogenesis in mammalian melanocytes and in melanoma cells which binds to a specific receptor on the cell surface, melanocortin-1 receptor (MC1-P), and induces activation of tyrosinase, the key enzyme for melanin formation, through stimulation of adenylate cyclase and protein kinase A [13]. α-MSH is of interest as a model for signal transduction effects from cyclic AMP up to the final product, in this case the quantifiable pigment melanin. It is already known that α-MSH can be covalently coupled to molecules using well-established procedures [14]. From an earlier study [14], it became clear that α-MSH coupled to PLL can be incorporated into multilayer films and that certain biological properties of such α-MSH derivatives remain active in this formulation. Recently, we have also shown that it is possible to use poly (L-glutamic acid) (PGA) as a carrier [15]. Furthermore, based on this PLL_{RP} gene delivery system, we simultaneously evaluated the melanin stimulation and gene expression in these cells by fluorescence microscopy. To further understand the bi-functionality, we labeled the SPT7pTL and PGA-α-MSH with YOYO-1 and Rhodamine, respectively, to follow its intracellular pathway by confocal microscopy.

2. Materials and methods

2.1. Materials

Poly (L-lysine) hydrobromide (PLL, $M_W = 30$ kDa) and poly-L-glutamic acid (PGA, 54 kDa) were purchased from Sigma. The SPT7pTL plasmid (5.3 kb) was grown in E. coli and purified by a Giagen kit (Qiagen, US). The purity and integrity of the plasmid were assessed by absorption spectroscopy (A_{260}/A_{280} ratio) and electrophoresis on a 1% agarose gel. The DNA concentration was determined by UV absorbance at 260 nm using a Cary 400 spectrophotometer.

2.2. PLL replica particle (PLL_{RP}) preparation and ζ-potentials characterization

PLL (or FITC-PLL) was infiltrated into porous silica particles at pH 8. After removing the excess PLL, the polypeptide was crosslinked within the silica particles using DMP (Sigma D8388), a homobifunctional crosslinker, which uses amine groups but does not remove the charges of the amine. The silica template particle was removed by aqueous HF buffered with ammonium fluoride to pH 5. The resulting PLL_{RP} (or FITC-PLL_{RP}) replica particles were washed with PBS until pH of the supernatant became equal to that of the fresh buffer [16,17].

For all the experiments, the particle distribution was measured by High Performance Particles Sizer (Malvern) instrument. The ζ-potentials were measured on a Zetasizer 2000 (Malvern) instrument.

2.3. PGA-α-MSH synthesis

The α-MSH was grafted to Maleimide-derivatized PGA as previously described [15].

2.4. Fluorescently labeled polyelectrolytes

Rhodamine B (Invitrogen, Cergy Pontoise, France) was coupled to PGA-α-MSH as previously described. The bis-intercalating agent YOYO-1 from Molecular Probes was added at a ratio of one dye for 300 bases of the SPT7pTL [18]. FITC-PLL was from Sigma (P3543), $M_W = 15$–30 kDa, with 0.3–1 mol% label.

2.5. Fluorescence imaging

The particles were imaged on an Olympus IX 71 inverted fluorescence microscope using a FITC filter.

2.6. Transmission electron microscopy

Transmission electron microscopy (TEM) (Philips CM 120 BioTWIN, operated at 120 kV) was used to examine the particle morphologies. The samples (2 μL) were placed onto Formvar-coated copper grids and allowed to air-dry.

2.7. Flow cytometry

Flow cytometry was performed on a Becton Dickson FACS calibur flow cytometry using excitation wavelength of 488 nm and 495 nm for YOYO-1 and FITC, respectively.

2.8. PLL_{RP}/(PGA-α-MSH + SPT7pTL) formation

First, PGA-α-MSH + SPT7pTL was prepared by mixing PGA-α-MSH with various amounts of SPT7pTL in equal volumes of phosphate buffered saline (PBS). Next, PLL_{RP}/(PGA-α-MSH + SPT7pTL) was formed by adding the PGA-α-MSH + SPT7pTL to various amounts of PLL_{RP} in equal volumes at room temperature by rotating for 15 min.

2.9. Cell cultures

Murine melanoma cells (B16-F1) were maintained at 37 °C in a humidified air-CO_2 (5%) atmosphere in modified minimum essential medium (MEM) with Earle's salts (Gibco, Paisley, UK) supplemented with 10% heat-inactivated fetal calf serum (FCS, Gibco), 2 mM L-glutamine, 1% MEM non-essential amino-acid solution, 1% MEM vitamin solution, 50 U mL^{-1} of penicillin and 50 μg mL^{-1} streptomycin [19].

2.10. Cell viability

Cell viability was evaluated by quantification of the cellular content in proteins. After treatment, the cells were washed three times in PBS and lysed by the addition of 100 μL of a cell lysis reagent (Promega). The cellular proteins were measured using the bicinchoninic acid assay (Interchim, Montlucon, France) following an incubation time of 30 min at 60 °C. The absorbance was recorded at 562 nm [20].

2.11. Melanin assay

The melanin content was quantified after 1, 2, and 3 days of incubation of cells with different chemicals. The cells were seeded in 24-well plates at 10,000 cells/well [19]. Optical densities (OD) of the supernatant were measured at 405 nm using an Elisa reader. Before each measurement the cell number was evaluated using a Neubauer counting chamber. OD was then normalized for each measurement to allow comparison between different culture conditions. The melanin content was evaluated according to a standard curve of melanin concentration. All experiments were performed at least three times, each yielding at least triplicate values.

2.12. Transfection protocols

For transfection, B16-F1 cells were incubated in complete medium with PLL_{RP}/(PGA-α-MSH + SPT7pTL), PGA-α-MSH + SPT7pTL, PLL_{RP}/SPT7pTL and free SPT7pTL. The amount of SPT7pTL used was 0.5 μg and 0.1 μg for these two cases (the number ratios of PLL_{RP} to cells were 500 and 100), respectively. After incubation, the transfection medium was removed and rinsed by PBS [21].

2.13. Immunofluorescence

B16-F1 cells were fixed with 2% paraformaldehyde in PBS for 4 min at room temperature and incubated twice for 10 min with PBS containing 0.1% Triton X-100 (PBS-Tx) [22]. After a PBS wash, the cells were incubated overnight at room temperature with primary antibody diluted at 1/1000 in PBS. Mouse polyclonal anti-SPT7 was used as the primary antibody. After overnight incubation at room temperature, the cells were washed with PBS-Tx and incubated with a fluorochrome-conjugated secondary antibody diluted at 1/500 in PBS-Tx for 1 h at room temperature. Cy3-conjugated goat anti-mouse (Jackson ImmunoResearch) was used as a secondary antibody. The cells were washed with PBS-Tx, rinsed with PBS, and counterstained with the Hoechst 33258 DNA dye (5 μg mL^{-1} bisbenzimide; Sigma) for 20 s. The cells were covered with mounting medium and analyzed by fluorescence microscopy.

2.14. Confocal laser scanning microscopy (CLSM)

A Bio-Rad MRC 1024 ES confocal microscope, with a Nikon Eclipse TE 300 inverted microscope, was used for the optical sectioning of cells. An argon/krypton mixed gas laser was used to illuminate a Nikon 60 × 1.2 NA water immersion objective. Emitted light was detected with two photomultipliers through selected band pass filters. Confocal sections were taken every 0.2 μm. Digital image recording was performed using the LaserSharp 2.3 software (Bio-Rad).

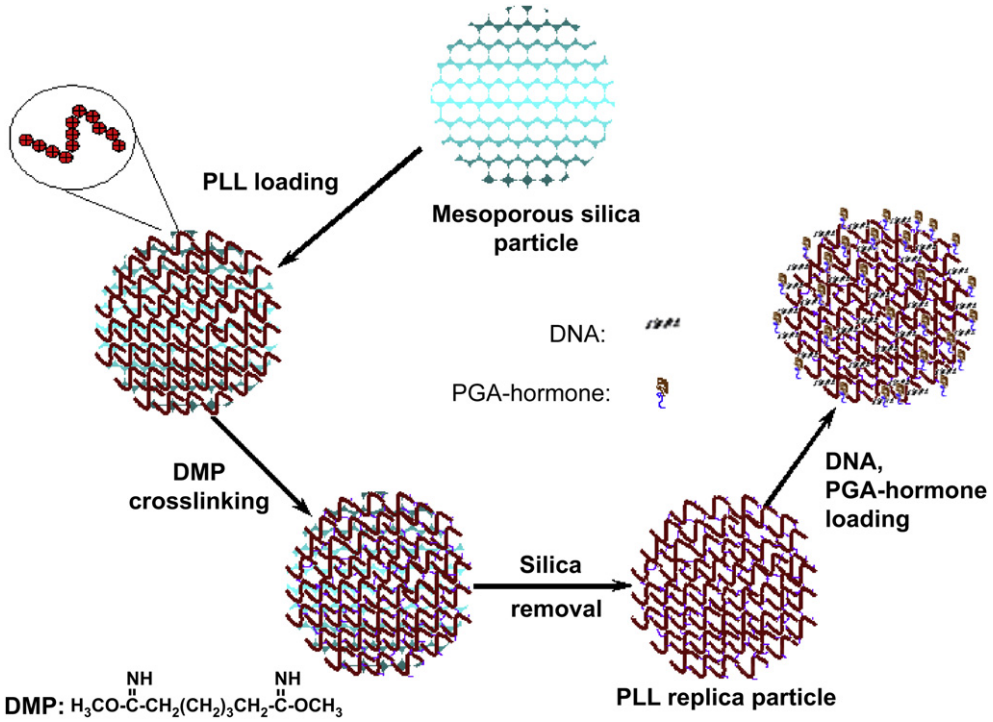

Scheme 1. Schematic illustration of the preparation of the poly(L-lysine) replica particles (PLL_{RP}) and cargo loading. PLL was infiltrated into mesoporous silica particles, crosslinked using a homobifunctional crosslinker and the template particles removed.

Excitation of YOYO-1 was achieved using the 488 nm excitation line, with the resulting fluorescent wavelengths observed using a 506–538 nm band pass filter (green). Rhodamine fluorescence was detected after excitation at 543 nm, and emission long pass filter 585 nm (red). All the experiments were performed in aqueous conditions [23].

3. Results and discussions

3.1. Characterization of PLL replica particles

The preparation of PLL_{RP} involved polymer infiltration into mesoporous silica (MS) particles, crosslinking of the adsorbed chains using a homobifunctional crosslinker and finally removal of the template particles [6]. This linker reacts with the substrate amine groups to form an amidine linkage which retains the positive charge (Scheme 1). The morphology of PLL_{RP} was analyzed by TEM (Fig. 1A) and visualized by fluorescence microscopy (Fig. 1B). The diameter of the PLL_{RP} measured by fluorescence microscopy was 2.5 μm, similar to that of the MS template particles. The diameter of the PLL_{RP} analyzed by TEM was ~1.5 μm, which is somewhat smaller than that derived from fluorescence microscopy. This size difference is attributed to the TEM measurements being conducted under vacuum. Using fluorescently labeled polymers and flow cytometry as a means to quantify the fluorescence of the particles, we established that $\sim 10^7$ PLL_{RP} particles contain 10 μg of the polypeptide, which effectively and near quantitatively adsorbs around 1 μg of nucleic acid and/or poly(L-glutamic acid) from their

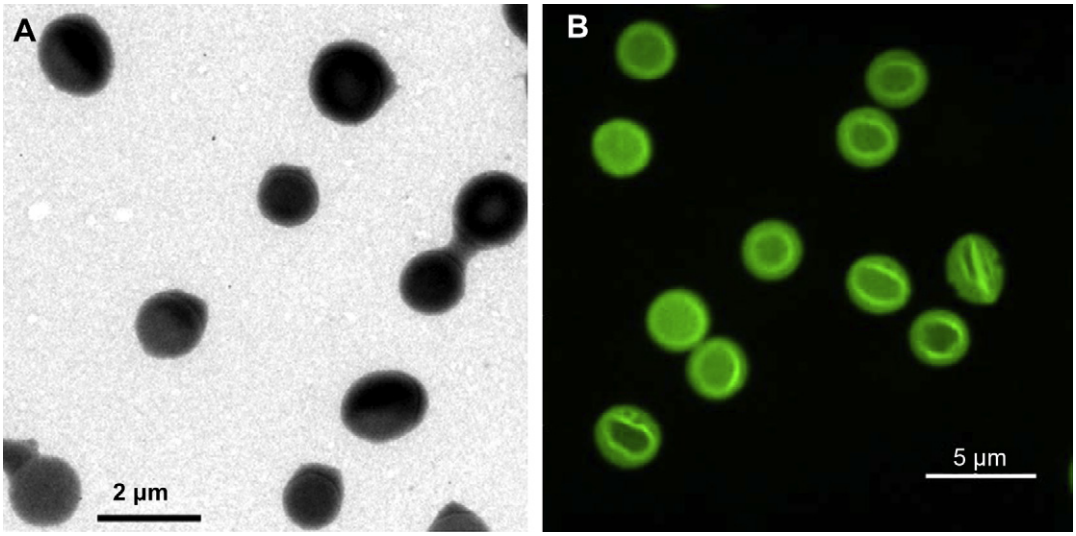

Fig. 1. TEM image of PLL_{RP} obtained by using MS porous silica template particles (A). Fluorescence image of PLL_{RP}. PLL_{RP} were fluorescently labeled with FITC (B).

solutions in phosphate buffered saline (1 mL) (Fig. 2). To characterize more the particles, we measured the zeta-potential of the loaded PLL_{RP} particles before and after adding the PGA derivative. We have shown that the PLL_{RP} particle has a zeta-potential of 21.5 mV. After PGA derivative loading, the zeta-potential of the particles decreased with the PGA derivative content increasing in the incubation solution. For instance, the PGA-loaded PLL_{RP} particles have a zeta-potential of 16.3 mV when incubated with 0.1 mg mL^{-1} and −20.2 mV when incubated with 1 mg mL^{-1} of PGA suggesting the success loading of the negatively charged cargoes on the positively charged PLL_{RP} particle.

3.2. Hormone stimulation and cell viability

The melanin secretion in the melanocytic cells was first monitored by the addition of various concentrations of free PGA-α-MSH after incubation for 1, 2 and 3 days (Fig. 3). The results showed that the PGA-α-MSH did not induce melanin production by cells after 1 day of incubation. However, after 2 days the melanin secretion significantly increased with increasing concentration of free PGA-α-MSH. Moreover, the melanin content reached a plateau when the concentration increased up to 0.02 μg mL^{-1}. After 3 days, the tendency of the melanin content was similar as that of 2 days.

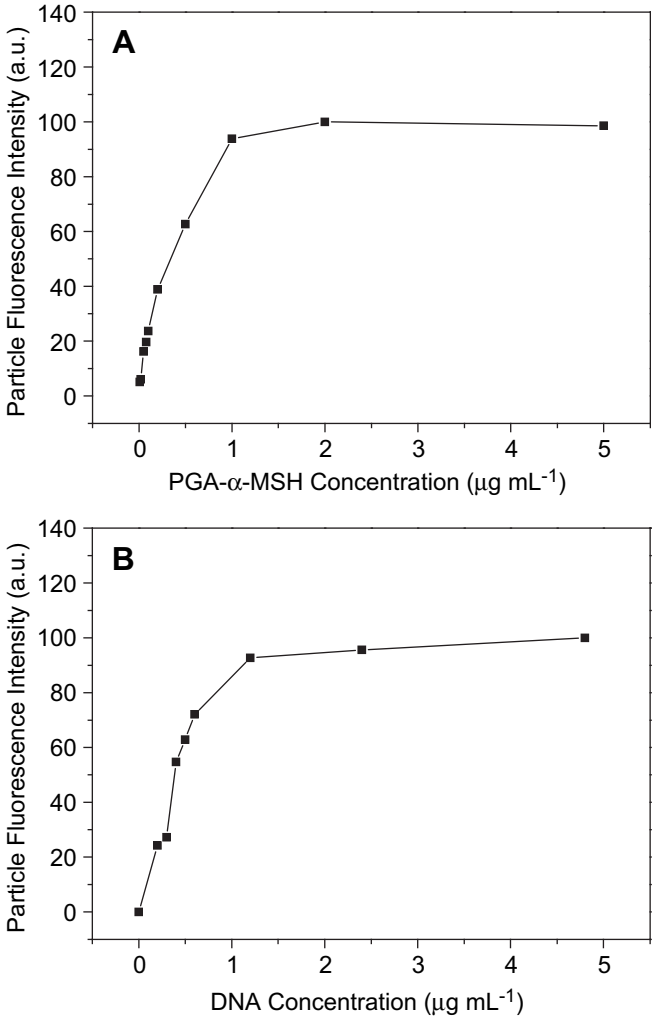

Fig. 2. Adsorption for PGA-α-MSH (A) and SPT7pTL (B) on PLL_{RP} particles. The data were obtained using fluorescently labeled PGA-α-MSH (FITC) and SPT7pTL (YOYO-1) and by using flow cytometry to quantify the fluorescence of the particles.

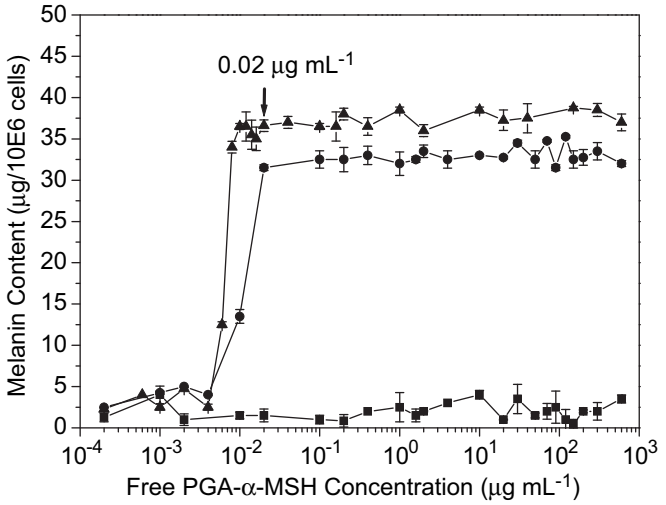

Fig. 3. Dose–response curves of B16-F1 melanoma cells to PGA-α-MSH. Cells were deposited on 24-well plates at a density of 10,000 cells/well. The melanin content was determined after 1 day (■), 2 days (●) and 3 days (▲) of stimulation with serial dilutions of PGA-α-MSH in three independent experiments.

Furthermore, the quantity of the melanin secretion for 3 days was slightly higher than that of 2 days.

The cell viability was also examined. For all cases, a high level of cell viability (≥90%) was found (Fig. 4). Since after 3 days incubation with free PGA-α-MSH the cells could secret a relatively high amount of melanin and do not significantly decrease the cell viability, a 3-day incubation period was taken as a suitable time all of the following experiments.

In a second step, the melanin secretion in cells was measured after incubation with the PLL_{RP}/PGA-α-MSH after 3 days. PLL_{RP}/PGA-α-MSH were prepared by mixing PGA-α-MSH with PLL_{RP} (500, 100, 10 and 1 PLL_{RP} per cell). The melanin content in the cells, which was measured by the addition of PGA-α-MSH at a concentration of 0.001 μg mL^{-1}, lower than the plateau concentration, was at the same level as the untreated cells (Fig. 5). This suggests that the melanin secretion in B16-F1 needs a certain amount of PGA-α-MSH to stimulate the melanogenesis. In the following experiments we

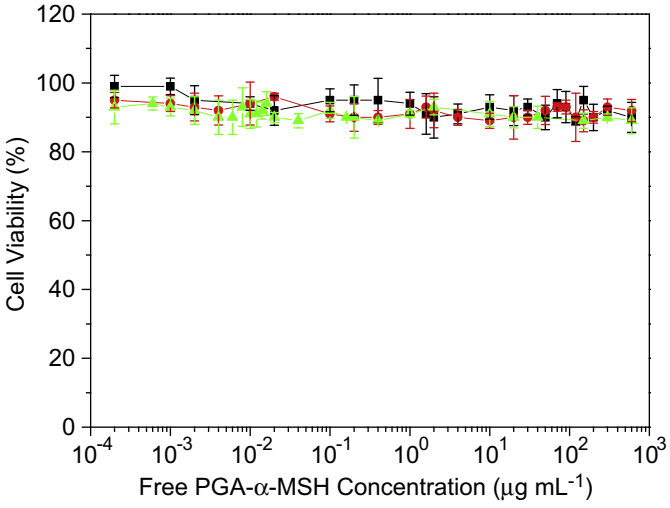

Fig. 4. Cell viability of B16-F1 cells incubated with PGA-α-MSH after 1 day (black, ■), 2 days (red, ●) and 3 days (green, ▲) was evaluated by determining the total protein amount per well of the treated cells relative to that of untreated cells. Experiments were carried out in triplicate.

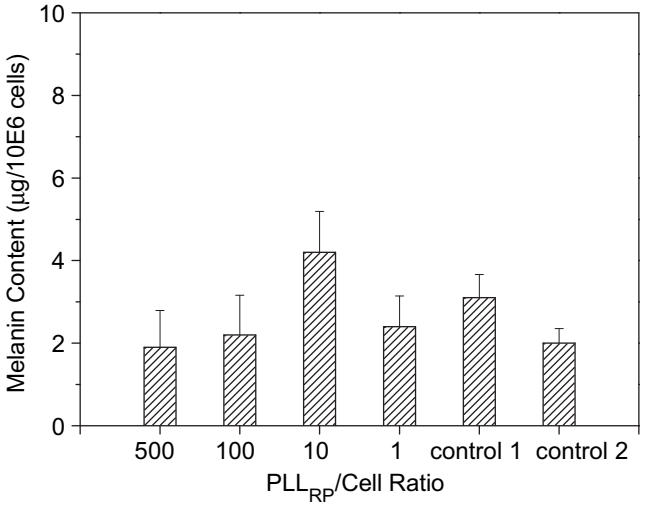

Fig. 5. Melanin production of B16-F1 cells. Cells were deposited on 24-well plates at a density of 10,000 cells/well. PLL_{RP}/PGA-α-MSH were prepared by mixing PGA-α-MSH with PLL_{RP} (500, 100, 10 and 1 PLL_{RP} per cell). The final concentration of PGA-α-MSH was 0.001 μg mL^{-1}. Control 1 and control 2 were free PGA-α-MSH and untreated cells, respectively. The melanin content was determined after 3 days of incubation with PLL_{RP}/PGA-α-MSH in three independent experiments.

chose a free PGA-α-MSH concentration of 0.02 μg mL^{-1}, which corresponds to a plateau concentration, where the melanin secretion of B16-F1 is stable.

In each case, the final concentration of PGA-α-MSH was 0.02 μg mL^{-1}, and for each sample, with the exception of a particle to cell ratio of 1:1, the PGA-α-MSH content was below PLL_{RP} saturation with adsorbed polypeptide (Fig. 6). That is, for a 500-, 100- and 10-fold excess of particles over the cells, the introduced PGA-α-MSH was adsorbed onto the surface of PLL_{RP}. From this figure, we found that the melanin secretion increased with increasing amount of PLL_{RP}, namely the PLL_{RP}/cell ratios. Accordingly, this suggests that PLL_{RP} not trouble the activity of PGA-α-MSH to stimulate the cellular melanin secretion. Furthermore, the cell

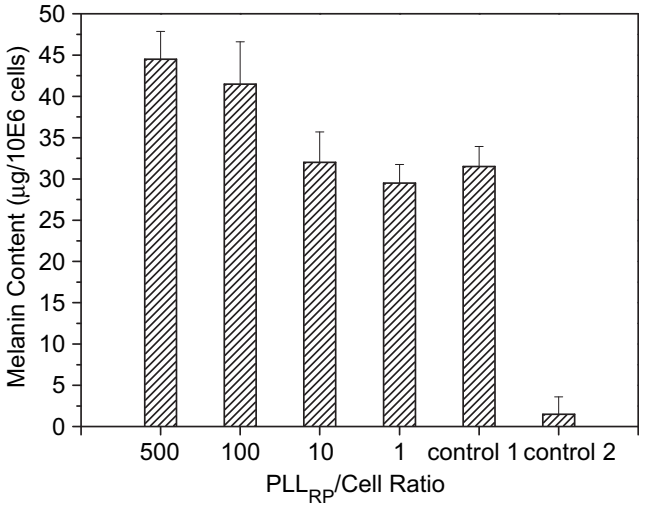

Fig. 6. Melanin production of B16-F1 cells. Cells were deposited on 24-well plates at a density of 10,000 cells/well. PLL_{RP}/PGA-α-MSH were prepared by mixing PGA-α-MSH with PLL_{RP} (500, 100, 10 and 1 PLL_{RP} per cell). The final concentration of PGA-α-MSH was 0.02 μg mL^{-1}. Control 1 and control 2 were free PGA-α-MSH and untreated cells, respectively. The melanin content was determined after 3 days of incubation with PLL_{RP}/PGA-α-MSH in three independent experiments.

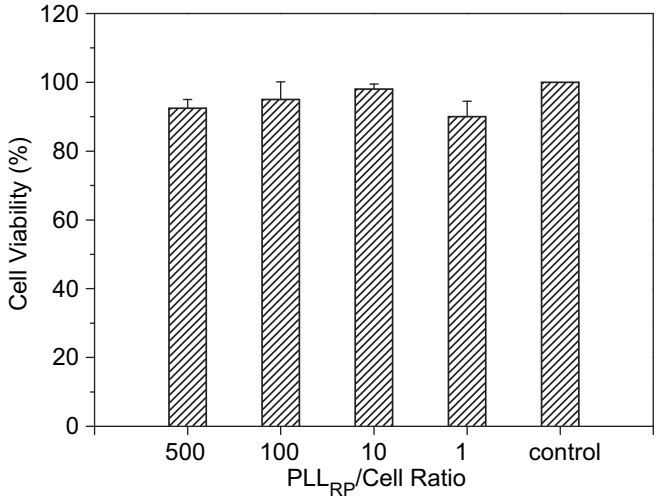

Fig. 7. Cell viability of B16-F1 cells incubated with PLL_{RP}/PGA-α-MSH was evaluated by determining the total protein amount per well of the treated cells relative to that of untreated cells. The control was the untreated cells. Experiments were carried out in triplicate.

viabilities in all these cases were high (≥ 90%) (Fig. 7). Therefore, we conclude that PLL_{RP} not only improves the melanin secretion but also does not contribute to the cytotoxicity.

3.3. Bi-functionality of PLL_{RP}

Since our aim was to evaluate the bi-functionality of PLL_{RP} as a gene delivery vector, we investigated the efficiency to deliver SPT7pTL into B16-F1 melanoma cells and melanin stimulation.

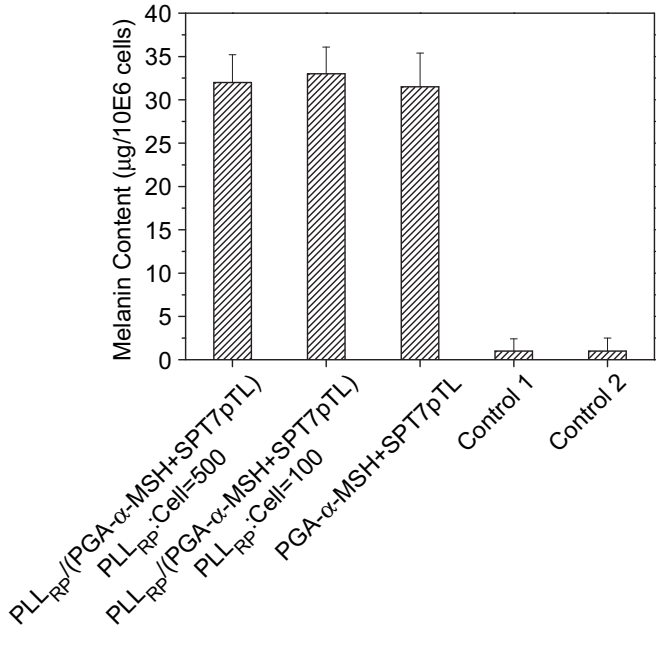

Fig. 8. Melanin production by B16-F1 cells. Cells were deposited on 24-well plates at a density of 10,000 cells/well. The concentration of PGA-α-MSH was 0.02 μg mL^{-1}. The amounts of PLL_{RP} were 500 and 100 particles per cell. Melanin content was measured after 3 days of incubation with PLL_{RP}/(PGA-α-MSH + SPT7pTL) and PGA-α-MSH + SPT7pTL, respectively. The controls 1 and 2 were PLL_{RP}/SPT7pTL and free SPT7pTL, respectively. The results are averages from three independent experiments.

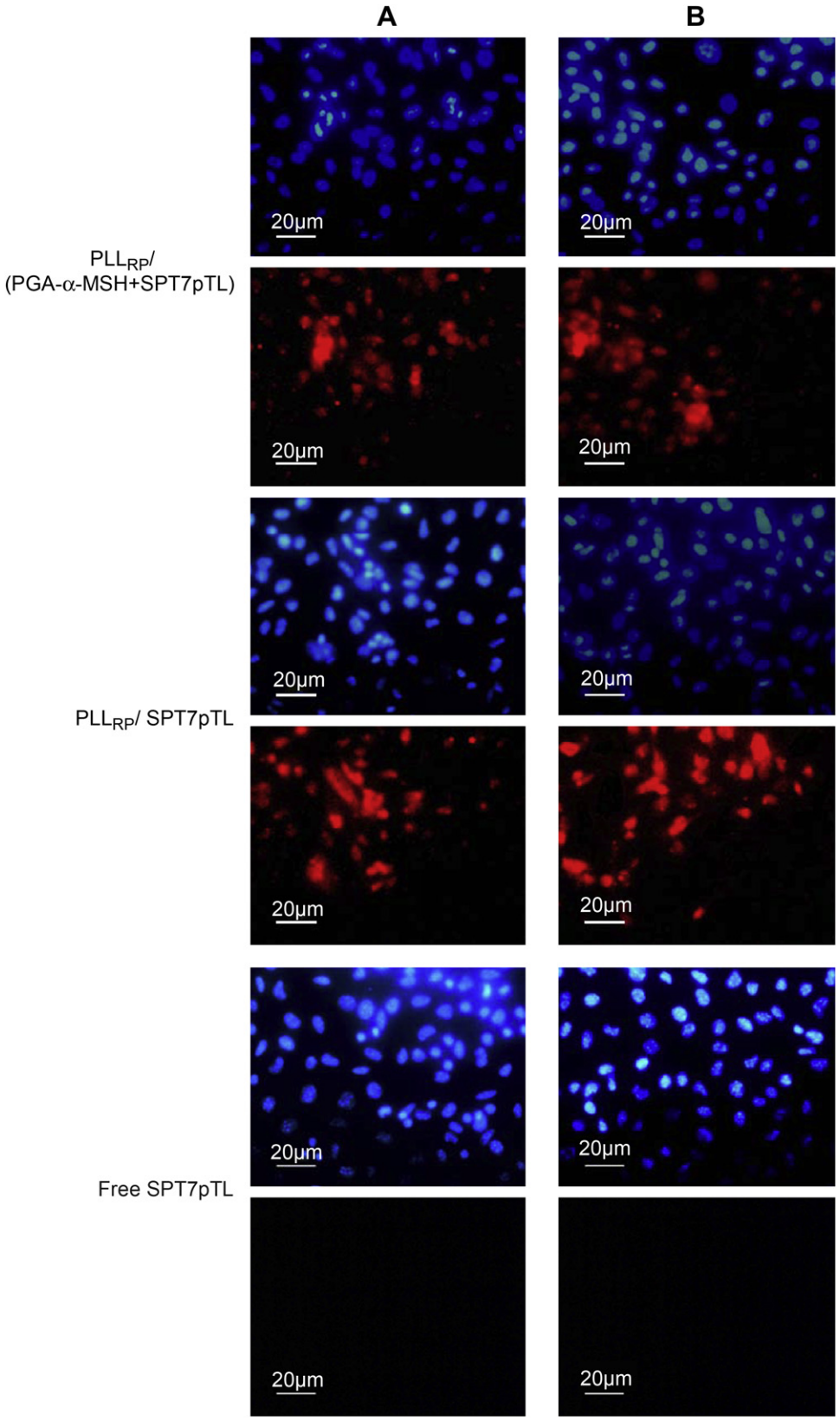

Fig. 9. Expression of SPT7 in B16-F1 cells for 3 days. The expression of SPT7 (red) was detected by using a mouse monoclonal anti-SPT7 as primary antibody and Cy3-conjugated goat anti-mouse as a secondary antibody. Nuclei were visualized by Hoechst 33258 staining (blue). The number of PLL_{RP} to cells was 500:1 (A) and 100:1 (B). Scale bars = 20 μm.

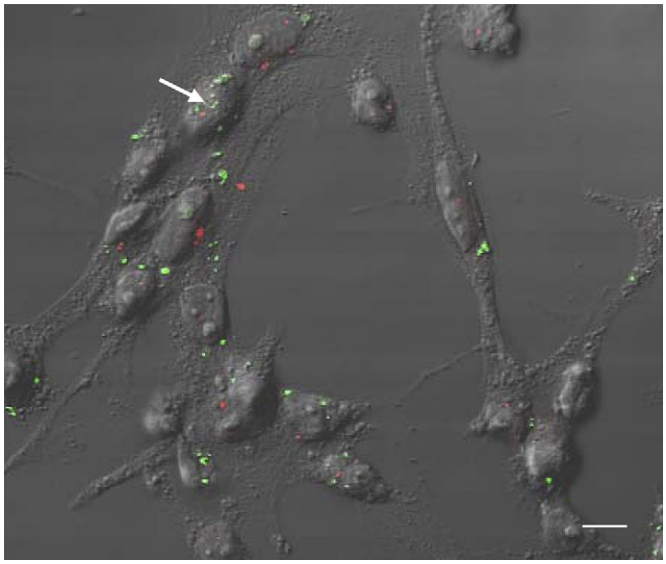

Fig. 10. Pathway of SPT7pTL and visualization of PGA-α-MSH in PLL_{RP}/(PGA-α-MSH + SPT7pTL) in the B16-F1 cells. The images correspond to the overlap of light transmission and fluorescence confocal images and were taken at 3 days post transfection. Red and green fluorescence correspond to areas containing Rhodamine-labeled PGA-α-MSH and YOYO-1 labeled SPT7pTL, respectively. The number ratio of PLL_{RP} to cells was 500. Images are representative of more than 90% of the observed cells. Scale bar = 20 μm.

Accordingly, in a next step, the melanin production was monitored after a 3-day incubation period with PLL_{RP}/(PGA-α-MSH + SPT7pTL) and PGA-α-MSH + SPT7pTL, respectively (Fig. 8). This study was performed at PLL_{RP} concentrations of 500 and 100 per cell. The melanin production of PLL_{RP}/(PGA-α-MSH + SPT7pTL) was not impaired and at the same level as that of PGA-α-MSH + SPT7pTL, approximately 20-fold higher than the controls. Furthermore, there were no significant differences in terms of melanin content for the various PLL_{RP} concentrations, which is in line with our previous study (Fig. 6).

The transfection ability of PLL_{RP} was next evaluated by expressing the human SPT7 nuclear transcription factor and the nuclei were visualized by Hoechst staining (Fig. 9). The gene expression was determined after 3-day incubation with PLL_{RP}/(PGA-α-MSH + SPT7pTL), PLL_{RP}/SPT7pTL and free SPT7pTL, respectively. The number ratios of PLL_{RP} to cells were 500 and 100. There was no gene expression in the case of free SPT7pTL, which is in line with the literature [19]. In contrast, in the case of PLL_{RP}/SPT7pTL, the gene expression of SPT7 in terms of cell number was significantly increased (~60–70%). For PLL_{RP}/(PGA-α-MSH + SPT7pTL), the gene expression was not impaired compared with PLL_{RP}/SPT7pTL. Furthermore, no obvious differences in gene expression were detected among the different ratios of PLL_{RP} to cells. Therefore, these data suggest that, as a gene delivery vector, PLL_{RP} could efficiently deliver SPT7pTL into melanocytic cells.

3.4. Intracellular pathway

To further follow the pathway of SPT7pTL molecules, and at the same time to understand the mechanism of the melanin secretion of the B16-F1 cells incubated with PLL_{RP}/(PGA-α-MSH + SPT7pTL) by confocal microscopy, the PGA-α-MSH and SPT7pTL were labeled with Rhodamine and YOYO-1 [24,25], respectively (Fig. 10). Since YOYO-1 is only fluorescent when it is intercalated in DNA, the pathway of the SPT7pTL could be monitored by green fluorescent spots. In Fig. 10, the small green spots were investigated in the nuclei (arrow) and in the cytoplasmic areas, which suggests that the DNA molecules were efficiently internalized into the nuclei. Simultaneously, Rhodamine-labeled PGA-α-MSH was seen as red spots in the cytoplasm and nuclear areas, which suggests that the PGA-α-MSH enters into the cell nuclei.

4. Conclusions

Our data suggests that the PLL_{RP} is a promising vector for gene therapy and hormone stimulation. PLL_{RP} is not cytotoxic. Moreover, PLL_{RP} could lead to efficient gene delivery and hormone stimulation followed by melanin production, simultaneously. The pathway of the DNA molecules was also visualized by confocal microscopy, and we found that SPT7pTL could enter into the nucleus. The entry of hormone into the cytoplasm and nuclei of cells induces melanin secretion.

Acknowledgments

This work was supported by the project ANR06-BLAN-0197-01/CartilSpray, from the "Agence Nationale de la Recherche", the "Fondation Avenir", the "Ligue contre le Cancer, du haut Rhin, Région Alsace" and "Cancéropôle du Grand Est". This work was also supported by the Australian Research Council under the Discovery Project and Federation Fellowship schemes, and by FAST. X.Z and C.M thanks the Faculté de Chirurgie Dentaire of Strasbourg for financial support. N.J is indebted to CHU de Nancy (Contrat d'interface vers l'hôpital). Supporting Information is available online from Wiley InterScience or from the author.

Appendix

Figure with essential colour discrimination. Fig. 4 in this article is difficult to interpret in black and white. The full colour image can be found in the online version, at doi:10.1016/j.biomaterials.2009.11.032.

References

[1] Duncan R. The dawning era of polymer therapeutics. Nat Rev Drug Discov 2003;2(5):347–60.
[2] Kataoka K, Harada A, Nagasaki Y. Block copolymer micelles for drug delivery: design, characterization and biological significance. Adv Drug Deliv Rev 2001;47(1):113–31.
[3] Torchilin VP. Recent advances with liposomes as pharmaceutical carriers. Nat Rev Drug Discov 2005;4(2):145–60.
[4] Edwards DA, Hanes J, Caponetti G, Hrkach J, Ben-Jebria A, Eskew ML, et al. Large porous particles for pulmonary drug delivery. Science 1997;276(5320):1868–71.
[5] Chong SF, Sexton A, De Rose R, Kent SJ, Zelikin AN, Caruso F. A paradigm for peptide vaccine delivery using viral epitopes encapsulated in degradable polymer hydrogel capsules. Biomaterials 2009;30:5178–86.
[6] Wang Y, Bansal V, Zelikin AN, Caruso F. Templated synthesis of single-component polymer capsules and their application in drug delivery. Nano Lett 2008;8(6):1741–5.
[7] Wang Y, Yu A, Caruso F. Nanoporous polyelectrolyte spheres prepared by sequentially coating sacrificial mesoporous silica spheres. Angew Chem Int Ed Engl 2005;44(19):2888–92.
[8] Wang YJ, Caruso F. Template synthesis of stimuli-responsive nanoporous polymer-based spheres via sequential assembly. Chem Mater 2006;18(17):4089.
[9] Wu GY, Wu CH. Receptor-mediated in vitro gene transformation by a soluble DNA carrier system. J Biol Chem 1987;262(10):4429–32.
[10] Ward CM, Read ML, Seymour LW. Systemic circulation of poly(L-lysine)/DNA vectors is influenced by polycation molecular weight and type of DNA: differential circulation in mice and rats and the implications for human gene therapy. Blood 2001;97(8):2221–9.
[11] Merdan T, Kopecek J, Kissel T. Prospects for cationic polymers in gene and oligonucleotide therapy against cancer. Adv Drug Deliv Rev 2002;54(5):715–58.
[12] Akinc A, Langer R. Measuring the pH environment of DNA delivered using nonviral vectors: implications for lysosomal trafficking. Biotechnol Bioeng 2002;78(5):503–8.

[13] Mountjoy KG, Robbins LS, Mortrud MT, Cone RD. The cloning of a family of genes that encode the melanocortin receptors. Science 1992;257(5074): 1248–51.
[14] Chluba J, Voegel JC, Decher G, Erbacher P, Schaaf P, Ogier J. Peptide hormone covalently bound to polyelectrolytes and embedded into multilayer architectures conserving full biological activity. Biomacromolecules 2001;2(3):800–5.
[15] Benkirane-Jessel N, Lavalle P, Meyer F, Audouin F, Frisch B, Schaaf P, et al. Control of monocyte morphology on and response to model surfaces for implants equipped with anti-inflammatory agents. Adv Mater 2004; 16(7):1507–11.
[16] Angelatos AS, Wang Y, Caruso F. Probing the conformation of polyelectrolytes in mesoporous silica spheres. Langmuir 2008;24(8):4224–30.
[17] Wang YJ, Alexandra SA, Dunstan DE, Caruso F. Infiltration of macromolecules into nanoporous silica particles. Macromolecules 2007;40:7594–600.
[18] Remy-Kristensen A, Clamme JP, Vuilleumier C, Kuhry JG, Mely Y. Role of endocytosis in the transfection of L929 fibroblasts by polyethylenimine/DNA complexes. Biochim Biophys Acta 2001;1514(1):21–32.
[19] Meyer F, Dimitrova M, Jedrzejenska J, Arntz Y, Schaaf P, Frisch B, et al. Relevance of bi-functionalized polyelectrolyte multilayers for cell transfection. Biomaterials 2008;29(5):618–24.
[20] Zhang X, Sharma K, Boeglin M, Ogier J, Mainard D, Voegel JC, et al. Transfection ability and intracellular DNA pathway of nanostructured gene-delivery systems. Nano Lett 2008;8(8):2432–6.
[21] Zhang X, Ercelen S, Duportail G, Schaub E, Tikhonov V, Slita A, et al. Hydrophobically modified low molecular weight chitosans as efficient and nontoxic gene delivery vectors. J Gene Med 2008;10(5):527–39.
[22] Benkirane-Jessel N, Oulad-Abdelghani M, Meyer F, Lavalle P, Haikel Y, Schaaf P, et al. Multiple and time-scheduled in situ DNA delivery mediated by beta-cyclodextrin embedded in a polyelectrolyte multilayer. Proc Natl Acad Sci U S A 2006;103(23):8618–21.
[23] Garza JM, Jessel N, Ladam G, Dupray V, Muller S, Stoltz JF, et al. Polyelectrolyte multilayers and degradable polymer layers as multicompartment films. Langmuir 2005;21(26):12372–7.
[24] Krishnamoorthy G, Duportail G, Mely Y. Structure and dynamics of condensed DNA probed by1,1′-(4,4,8,8tetramethyl-4,8-diazaundecamethylene)bis[4-[[3-methylbenz-1,3-oxazol-2-yl]methylidine]-1,4dihydroquinolinium] tetraiodide fluorescence. Biochemistry 2002;41(51):15277–87.
[25] Krishnamoorthy G, Roques B, Darlix JL, Mely Y. DNA condensation by the nucleocapsid protein of HIV-1: a mechanism ensuring DNA protection. Nucleic Acids Res 2003;31(18):5425–32.